ELSEVIER

Journal of Nuclear Materials 266–269 (1999) 819–824

journal of nuclear materials

# Transport properties of hydrogen isotopes in boron carbide structures

A.A. Grossman [a,*], R.P. Doerner [a], S. Luckhardt [a], R. Seraydarian [a], A.K. Burnham [b]

[a] *Fusion Energy Research Program, University of California, San Diego, Mail Code 0417, 9500 Gilman Drive, La Jolla, CA 92093-0417, USA*

[b] *Lawrence Livermore National Laboratory, Livermore, CA 94551, USA*

**Abstract**

The transport of implanted hydrogen isotopes in the refractory semiconducting ceramic, boron carbide, is investigated using the TMAP4 code. A review of experimental results for the diffusivity and solubility of hydrogen isotopes in boron carbide is presented, which provide Arrhenius expressions for the kinetics of hydrogen isotope transport. These expressions are utilized in the TMAP4 model to provide predictions for the hydrogen isotope implantation and desorption for experiments now in progress at the UCSD PISCES laboratory for the National Ignition Facility (NIF). © 1999 Elsevier Science B.V. All rights reserved.

*Keywords:* Thermal deposition; Hydrogen diffusion; Boron carbide; Hydrogen retention

## 1. Introduction

In the proposed National Ignition Facility (NIF), inertial fusion targets are to be imploded using high energy laser pulses. These implosion events typically are accompanied by intense bursts of soft X-rays which will heat the surface of the chamber wall. Moreover target debris, including gaseous and ionized tritium will also impinge on the heated surface. Boron carbide is a refractory ceramic being evaluated for use as a first wall material in this environment. A major concern is the retention and permeation of tritium implanted into this plasma facing surface. Laboratory-scale experiments are under way to investigate mechanisms that influence hydrogen isotope transport and retention in a variety of specimens of this material.

The principal question is: if the surface of boron carbide is heated to a temperature of 2000°C and the temperature depth profile is exponential with a scale size of 1 μm, will the implanted deuterium (which is implanted to a depth of 1 μm) be activated and diffuse out of the material? This problem is proposed in the context of tritium retention in the NIF first wall [1,2], but is also of interest to other areas where the transport of hydrogen isotopes in boron carbide is important, such as magnetic fusion plasma facing components, re-processing of fission reactor fuel, and direct thermoelectric power generation.

## 2. Model

To address this issue, a model using the TMAP4 code [3] was developed to analyze hydrogen isotope implantation and desorption in boron carbide. The movement of dissolved hydrogen isotopes in boron carbide is solved using the conservation of atoms law, the diffusive flux, and the action of trapping, in one space dimension. Because the processes that govern permeation of the solute lattice gas are all strongly temperature dependent via Arrhenius' Law, the time-dependent heat conduction equation for the thermal response of the solid structure is also solved. The main input assumed only a single species is present in the material, atomic deuterium,

* Corresponding author. Tel.: +1-619 534 9712; fax: +1-619 534 7716; e-mail: grossman@fusion.ucsd.edu.

0022-3115/99/$ – see front matter 
PII: S0022-3115(98)00517-0

denoted by D. Outside the material is assumed that only molecular deuterium, $D_2$, is present in the two enclosures. The material is represented as a single segment with 54 nodes. The enclosures are treated as a boundary enclosure, which represents static condition environments that are not altered by heat transfer or diffusion effects. The enclosure temperature, which is used by TMAP4 to relate pressure and enclosure species concentration, was taken to be 30°C. During the implantation calculation, the $D_2$ species partial pressure in the enclosure was specified to be $10^{-3}$ Torr, regardless of whether the implantation source was on or off. The geometric structure of the problem was further specified by selecting a set of node separations, $\Delta x$, used in the finite difference representation of both the heat and mass diffusion equations, to provide submicron resolution in the implantation region (see Fig. 1) and coarser resolution elsewhere, and were chosen to be 0.0, $15(10^{-7})$, $3(3 \times 10^{-5})$, $31(3 \times 10^{-4})$, 0.0 m for a total thickness of 9.4 mm, where the left and right-most nodes provide boundary conditions and are required to have zero thickness. During the implantation phase calculation, all the nodes were taken to be initially at room temperature,

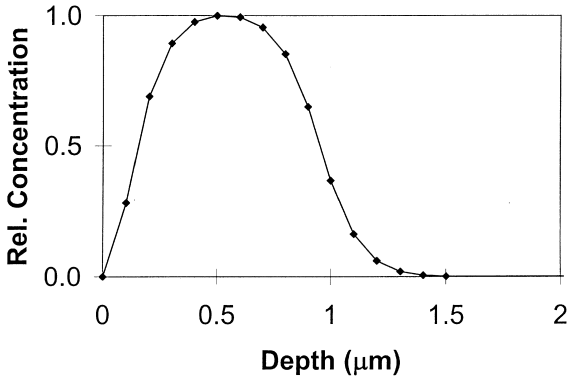


Fig. 1. Mobile concentration vs. depth, as calculated by TMAP4 at the end of the implantation calculation (at the end of the sample cool down to room temperature).

and the temperature of the surface node was specified to be as reaching a temperature of 523 K within 60 s of plasma bombardment, and held there for another minute then allowed to cool to room temperature in 1 h after plasma bombardment. The thermal conductivity was taken to be 400 W $m^{-1}$ $K^{-1}$, and the specific thermal capacity was taken to be [4]

$$C_p(\text{cal/mol K}) = 22.99 + 5.40 \times 10^{-3} T - 10.72 \times 10^{5} T^{-2}$$

which is then used by TMAP4 to calculate the temperature at each of the nodes for the specified surface temperature. For the mass diffusion part of the problem, the initial concentration of the solute is taken to be zero, the optional trapping was turned off, and the diffusivity specified to be an Arrhenius relation with given activation energy and prefactor. The source term in the mass diffusion equation represents the implanted D, and was taken to be an order of magnitude smaller than the flux incident on the sample, a consequence of the saturation effect. The source peaking factor was taken to be unity on each of the first 10 nodes covering 1 μm, and zero thereafter. For the boundary condition, the TMAP4 lawdep option was used, which specifies that concentration of the diffusion species in the surface node is controlled by a Sievert's solution law. The solubility constant was specified to obey an Arrhenius relation with specified activation energy and prefactor. Both the diffusivity and solubility are key parts of the model, and are empirically determined. A review of the scientific literature having these key data is therefore necessary before a TMAP4 model can be used to produce meaningful results. The most significant papers are briefly summarized in the next section and in Tables 1 and 2; additional information can be found in Ref. [5].

## 3. Hydrogen kinetics in boron carbide

There are thousands of papers in the scientific literature on hydrogen diffusion, solubility and permeation

Table 1
Diffusion activation energies and diffusivity prefactors of tritium in boron carbide

| Reference | $E_A$ (kJ/mol) | $D_0$ ($cm^2/s$) |
|---|---|---|
| Elleman et al. (1978) [17] | 70 ± 7 | $1.1 \times 10^{-6}$ |
| Schnarr, Munzel (1990b) [11] | 87 ± 10 | $6.67 \times 10^{-5}$ |
| Schnarr, Munzel (1990a) [10] | 95 ± 10 | $1.5 \times 10^{-4}$ |
| Braganza (1978a) [12] | 193.3 | $1.24 \times \sqrt{\frac{2}{3}} \times 10^{-2}$ |
| Suhaimi et al. (1986) [19] | 196 ± 10 | $2.67 \times 10^{1}$ |
| Schnarr, Munzel (1990c) [11] | 210 ± 10 | $6.54 \times 10^{1}$ |
| Braganza (1978b) [12] | 229.4 | $1.37 \times \sqrt{\frac{2}{3}} \times 10^{-2}$ |
| Miles et al. (1974) [21] | 235 ± 30 | – |
| Gidarakos (1984) [20] | 250 ± 30 | – |
| Braganza (1978c) [12] | 377 | $1.37 \times \sqrt{\frac{2}{3}} \times 10^{-2}$ |

Table 2
Temperature ranges of thermal desorption studies in boron carbide, and projected diffusivity of deuterium at 2000°C

| Reference | Temperature range (°C) | $D^{projected}$ (2000°C) ($cm^2/s$) |
|---|---|---|
| Elleman et al. (1978) [17] | 300–700 | $3.3 \times 10^{-8}$ |
| Schnarr, Munzel (1990a) [10] | 400–800 | $1.2 \times 10^{-6}$ |
| Schnarr, Munzel (1990b) [11] | 500–900 | $8.2 \times 10^{-7}$ |
| Schnarr, Munzel (1990c) [11] | 500–900 | $1.2 \times 10^{-3}$ |
| Suhaimi et al. (1986) [19] | 550–680 | $1.0 \times 10^{-3}$ |
| Miles et al. (1974) [21] | 700–900 | – |
| Gidarakos (1984) [20] | 600–750 | – |
| Braganza (1978a) [12] | 300–1700 | $4.5 \times 10^{-7}$ |
| Braganza (1978b) [12] | 300–1700 | $7.5 \times 10^{-8}$ |
| Maruyama and Iseki (1985) [22] | 500–900 | – |
| Franzen et al. (1992) [23] | 300–1100 | – |
| Yamuchi et al. (1995) [24] | 0–1100 | – |

through metals. For non-metallic substances, there are far fewer papers available, mainly on hydrogen transport in metallic oxides, hydrated salts, graphites, and some semiconductors, such as silicon and germanium. In general, very few papers exist for the nitrides, halides, and carbides. Of these, most are restricted to diffusion coefficients; almost no attention is paid to solubility or overall permeability. In metals, the mobility of the hydrogen isotopes is very high. A common value for the diffusivity at 600°C for metals is given by $D = 10^{-4}$ $cm^2$ $s^{-1}$. The reason for this high degree of mobility is that in metals, the molecular form of hydrogen is not present, only the atomized state. Moreover the high conductivity of metals implies that the atomic hydrogen is stripped of its electron, and the moving species is a small and very mobile proton, deuteron, or triton.

Boron carbide's specific resistivity is nominally 0.5 Ω cm at 25°C which places it among the semiconductors. Boron carbide is a high temperature ceramic which is often used in reactor technology as a neutron absorber, which produces hydrogen in the material, so studies do exist of its hydrogen diffusion and thermophysical properties. These studies indicate that the thermophysical properties of boron carbide depend very little on the specific method of production but do depend strongly on the stoichiometric composition. The name boron carbide was assigned the stoichiometric formula $B_4C$ when it was patented as an abrasive in the 1930s. However, what is termed boron carbide can actually refer to a wide phase homogeneity range $B_4C$–$B_{10.5}C$ and depending on this composition some of these boron carbides can have conductivities many orders of magnitude larger, and undergo metal–insulator transitions [6]. The possibility that implantation can change the surface composition has been explored and it is also observed to affect the hydrogen retention [7]. The diffusivities and solubilities of hydrogen isotopes in boron carbide as well as other thermophysical properties are determined by the structural features. The most widely accepted representation [8] is the remarkable close packed rhombohedral lattice (lattice constants $a = 5.19$ Å and $\alpha = 66°18'$) consisting of $B_{11}C$ icosahedra interconnected by C–B–C intericosahedral chains (hexagonal lattice parameters $a_H = 5.608$ Å, $C_H = 12.088$ Å). The bonds are strongly covalent, with intericosahedral bonds strong or stronger than the intra-icosahedral bonds because the distance between the icosahedrons is less than that between the atoms in the icosahedron. This unusual structure accounts well for the observed physical properties of great hardness and appreciable electrical conductivity. It was also recognized early on that this structure allows room for accommodation of additional atoms, suggesting that boron carbide with B/C ratio greater than 4 is a solid solution. The rhombohedral framework encloses two holes per unit cell, each large enough to accommodate an extra atom. It is these holes that are thought to serve as the interstitial sites for hydrogen. With this assumption, it is possible to use a dilute solution model [9] to analyze hydrogen solubility in boron carbide. This is the first step on obtaining information on the thermodynamics of hydrogen in boron carbide, which is needed for a clear understanding of the experimental observations of diffusion, chemical erosion, hydrogen retention and thermal desorption. In the following we summarize the key results for diffusivity (see also Tables 1 and 2) and solubility which are utilized in the present TMAP4 model.

The release of tritium from boron carbide powder and a single crystal was investigated by Schnarr and Munzel [10,11], in the temperature range 400–800°C. The samples were prepared with a uniform tritium distribution with high energy tritons produced by bombarding a Cu target with 104 MeV alpha particles. They also investigated the release of tritium from the sintered material with densities of 70–95% of the theoretical density, as well as the release from preoxidized samples. Under the assumption that diffusion within the boron carbide is the rate controlling step and that the effective

average grain size can be deduced from the specific surface area of the power, they found an activation of 95 ± 10 kJ mol$^{-1}$.

Boron carbide is used in control rods of nuclear reactors because of its large neutron absorption cross-section. For thermal neutrons, the reaction $^{10}B(n,\alpha)^7Li$ has a cross-section of 3840 b, decreasing to 200 mb for 1 MeV neutrons. A very important side reaction which forms tritium is $^{10}B(n,2\alpha)^3H$, which has a neutron threshold energy of 1 MeV and has a cross-section that increases to 200 mb with increasing neutron energy. Schnarr and Munzel [11] addressed the issue of tritium retention from irradiated boron carbide. They found that the effective diffusion coefficient decreases by three orders of magnitude with increasing total neutron dose, and attributed this decrease in tritium mobility to the radiation defects formed in the boron carbide. At a high dose of neutrons of $3.5 \times 10^{18}$ n/cm$^2$ from a heavy water reactor, they found an activation energy of 210 ± 30 kJ mol$^{-1}$ in the irradiated material, which was much higher than in the low-dose and unirradiated material. The low doses used 22 MeV neutrons with a dosage of about $10^{16}$n/cm$^2$, for which they found an activation energy of 87 ± 10 kJ mol$^{-1}$. At this activation energy, the release at room temperature is very small (less than 1% over the lifetime of the tritium). On the other hand, temperatures of >1000°C are required to remove, in only a few hours, more than 90% of the tritium from boron carbide irradiated with approximately $10^{19}$ n/cm$^2$.

The activation energies for desorption of atomic deuterium on unirradiated boron carbide were obtained by Braganza [12], using thermodesorption with a linear heating schedule. Two peaks were observed in boron carbide, these were for temperatures below 925°C, and a rise in thermodesorption signal above that temperature was associated with the absorpton of atomic D in the bulk of the material. The adsorption of deuterium from a molecular state was observed to be very slow, and a tungsten filament was used to predissociate the molecular deuterium to increase the rate of adsorption. This justified the use of second order kinetics to analyze the desorption spectra, since if the molecules are dissociatively adsorbed, desorption must involve the surface collision of two atoms. The general rate equation is $dn/dt = n^2k^2\exp(-E/RT)$, where $n$ is the coverage in mols/cm$^2$, $k^2$ is the rate constant in cm$^2$/s, $E$ is the activation energy for desorption in kcal/mol, $T$ is the target temperature in K. Using the analysis of Redhead [13], for a linear heating schedule of the form, $T = T_0 + \beta t$, the activation energy at the peak temperature is $E = 4(N\mathrm{p}/\sigma_0\beta)RT_\mathrm{p}^2$. This equation illustrates that it is the activation energy that is the physical property of the material, rather than the location of the temperature (which depends on the ramp rate). The first peak for boron carbide occurred at 710°C, and the activation energy was found from this equation to be 193.4 kJ mol$^{-1}$. The second peak occurred at 880°C and its activation was calculated to be 267.4 kJ mol$^{-1}$. Release from a higher temperature site started, occurring for temperatures greater than 1427°C. The two peaks could only be resolved for low doses of atomic deuterium, at $2 \times 10^{19}$ atoms/cm$^2$. For higher doses, atomic deuterium was preferentially adsorbed at the high temperature site of 880°C. The high temperature desorption at 1427°C corresponds closely to an activation energy in the region of 377 kJ mol$^{-1}$, which represents the bulk dissociation energy for a B–H bond. The last peak beyond 1427°C was not fully resolved (the required temperature was too high), but it is significant if temperatures of 2000°C are desired. This illustrates that the breaking of any chemical bonds between C–H may begin to occur and produce additional high temperature peaks in the desorption spectra that would not be anticipated on the basis of the lower temperature measurements that are more commonly used. The chemical bond activation energies between hydrogen and boron carbide are found in the papers by Steck et al. [14] and Booth and Ache [15].

Elleman et al. [16–18] used boron carbide samples that were doped with tritium in a surface layer about 20 μm thick. Tritium was produced by the reaction of thermal neutrons via $^6Li(n,\alpha)^3H$. The neutron dose was $2 \times 10^{14}$ n/cm$^2$, a relatively low radiation dose, which implies that the determined diffusion coefficients are characteristic for tritium mobility in unirradiated material. The activation energy is 70 ± 7 kJ mol$^{-1}$, which is relatively low for boron carbide and consistent with the claim that it applies to the unirradiated material.

Suhaimi et al. [19] used boron carbide samples exposed to neutrons with an average energy of 6.5 MeV and a dose of $10^{14}$ n/cm$^2$, which is a low radiation dose, and imply that the determined diffusion coefficients are applicable to the unirradiated material. The reported activation energy is 196 ± 30 kJ mol$^{-1}$, which is high and more typical of radiation damaged material.

The only solubility data for hydrogen in boron carbide found in the literature are the TDS measurements of Shirasu et al. [9]. That data closely obeyed the Sievert's solubility law, indicating that the deuterium is in atomic form in the boron carbide. The temperature dependence of Sievert's constant, $K_\mathrm{H}$, obeys an Arrhenius relationship: $\ln K_\mathrm{H} = A + \{B/T\}$ the values of $A$ and $B$ were estimated as −15.6 and 3570. This latter value corresponds to an enthalpy of solution of −29.7 kJ mol$^{-1}$, the negative sign indicating that hydrogen dissolves exothermically in boron carbide.

## 4. Model results

The Arrhenius plots of each of the above diffusivities are given in Fig. 2. It is seen there are orders of mag-

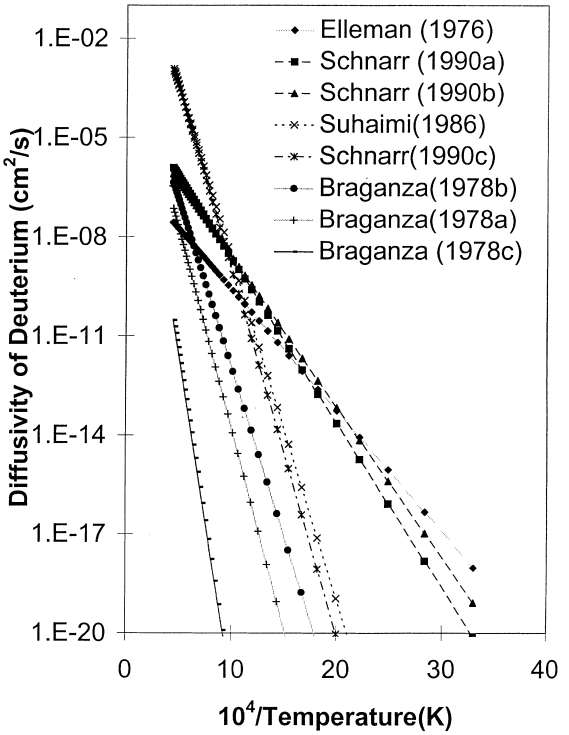


Fig. 2. Comparison of the Arrhenius relations for diffusivities of deuterium in boron carbide used in the calculation shown in Figs. 1 and 3. Note that metals have diffusivities that are many orders of magnitude larger.

nitude differences between the diffusivities. High dose radiation damaged boron carbide tend to have large activation energies, and low diffusion prefactors. Unirradiated and low dose radiation damaged boron carbide tends to have smaller activation energies and larger diffusion prefactors. Chemical bonding of hydrogen to the boron carbide can also yield very large activation energies. The values for the diffusivity at a given temperature in boron carbide are many orders (four and more) smaller than in metals. They are also orders of magnitude larger than most non-conductors, consistent with boron carbide's status as a semiconductor. The diffusivity is extremely small at room temperatures, so at that temperature hydrogen is immobile in boron carbide. At the highest temperatures (2000°C), the projected diffusivity approaches that of many common metals at 600°C for two of the models, the rest are still orders of magnitude smaller.

Using these diffusivities, and the one available solubility, the implantation TMAP4 model described in the first section was run, using a surface temperature and implantation schedule that has been used in the past by PISCES. The TMAP4 results for the mobile concentration of deuterium at the end of the implantation calculation were found peak inside the surface, then exponentially decrease from the peak over a micron depth scale, and was negligible through the rest of the bulk, see Fig. 1. The overall shape is comparable to the concentration depth profile observed for deuterium implantation in boron carbide by Jimbou et al. [7].

A desorption phase calculation was set up as a restart run from the implantation calculation. The temperature schedule is a linear ramp to 2000°C. A restart run was done for each of the diffusivities found in the literature, and the surface flux data extracted as a function of time from the TMAP4 output. A negative surface flux denotes a desorption flux, a positive flux would indicate absorption. The deuterium gas pressure was programmed to be constant at $10^{-3}$ Torr throughout. The results are summarized in Fig. 3 which plots the desorbed surface flux and the linear temperature ramp vs. time, and in Fig. 4 which plots the desorbed surface flux vs. temperature. Qualitatively the results are similar to that obtained experimentally, single well defined peaks of desorption at relative locations seen in the literature. For example, the two low temperature peaks of Braganza [12] are distinguishable, and the lower temperature peak occurs with the diffusivity given for that peak, similarly for the higher temperature peak. The highest temperature peak is the one Braganza [12] attributed to the breaking of chemical bonds. Ignoring that one, then

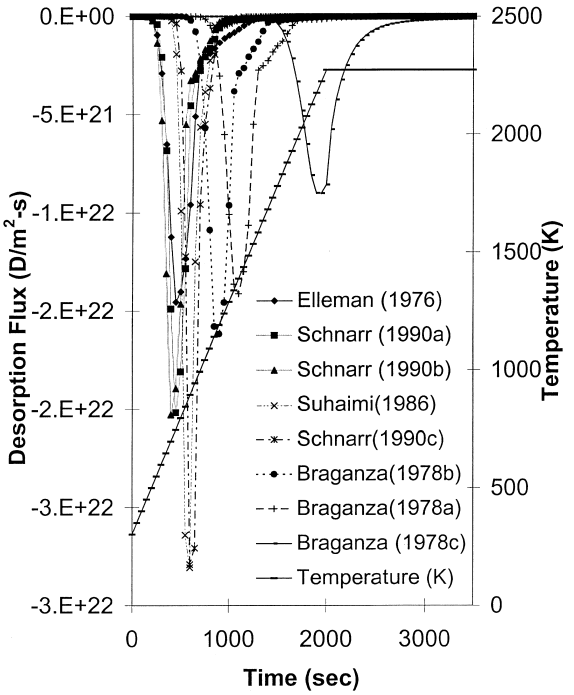


Fig. 3. TMAP4 desorption flux vs. time for deuterium from boron carbide using Elleman et al. [16–18], Schnarr and Munzel [10,11], Suhaimi et al. [19], and Braganza [12] diffusivities. Also shown is the linear temperature ramp.

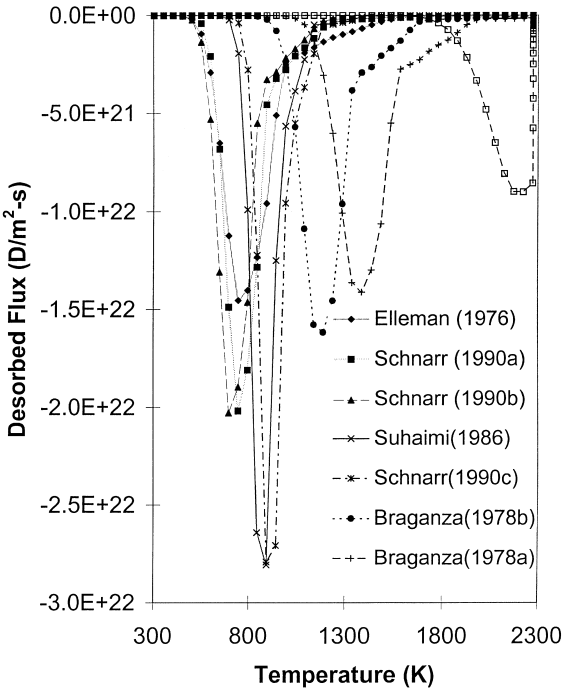


Fig. 4. TMAP4 desorption flux vs. temperature for the diffusivities plotted in Fig. 2.

all the peaks clearly occur well below the 2000°C. Even though there are order of magnitude differences in the diffusivities over the entire range of temperatures (30–2000°C), many of the peaks coincide, or occur, at a common temperature. Looking back at the Arrhenius plots suggests how this occurs – the lines cross in the temperature regime where the peaks are expected to occur. In the case of Braganza [12], whose Arrhenius plots either do not cross or cross at the highest temperatures, then the desorption peaks occur at distinctly different temperatures. Comparing the mobile inventory at the beginning and end of the desorption calculation shows it is down by at least an order of magnitude. This observation indicates that 90% of the hydrogen is desorbed with this temperature ramp, or put another way, that only 10% of the retention from the previous NIF shot would be expected to accumulate in the wall after a subsequent implosion.

## References

[1] A.K. Burnham, C.S. Alford, D.M. Makowiecki et al., Fusion Technol. 31 (1997) 456.
[2] A.K. Burnham, M.T. Tobin, A.T. Anderson et al., Fusion Technol. 30 (1996) 730.
[3] G.R. Longhurst, D.F. Holland, J.L. Jones, B.J. Merrill, EGG-FSP-10315, Idaho National Engineering Laboratory, June 12, 1992.
[4] F. Thevenot, J. European Ceram. Soc. 6 (1990) 205.
[5] A. Grossman, UCSD-ENG-037 and UCSD-ENG-053, Fusion Energy Research Program, University of California, San Diego, 1997.
[6] H. Werheit, K. DeGroot, W. Malkemper, J. Less-Common Meta. 82 (1985) 153.
[7] R. Jimbou, N. Ogiwara, M. Saidoh et al., J. Nucl. Mater. 220–222 (1995) 869.
[8] H.K. Clark, J.L. Hoard, J. Am. Chem. Soc. 65 (1943) 2115.
[9] Y. Shirasu, S. Yamanaka, M. Miyake, J. Alloys Compounds 190 (1992) 87.
[10] K. Schnarr, H. Munzel, J. Chem. Soc. Faraday Trans. 86 (1990a) 651.
[11] K. Schnarr, H. Munzel, J. Nucl. Mater. 170 (1990b,c) 253.
[12] C.M. Braganza, Vacuum 29 (1978a,b,c) 73.
[13] P.A. Redhead, Vacuum 12 (1962) 203.
[14] S.J. Steck, G.A. Pressley, Jr., F.E. Stafford, J. Phys. Chem. 73 (1969) 1000.
[15] T.E. Booth, H.J. Ache, J. Nucl. Mater. 84 (1979) 85.
[16] T.S. Elleman, C. Alexander, R. Causey et al., Proc. Meeting on CTR Electrical Insulatory, Los Alamos, 1976 CONF-76 0558, 1976, p. 163.
[17] T.S. Elleman, L.R. Zumwalt, K. Verghese, Proc. 3rd Top. Meeting on Tech. Controlled Nuc. Fus. vol. 2, Santa Fe, NM, CONF-780508, 1978, p. 763.
[18] T.S. Elleman, D. Rao, K. Verghese, L. Zumwalt, Hydrogen Diffusion, Dissolution and Permeation of Nonmetallic Solids, ORO-4721, 1979.
[19] A. Suhaimi, R. Wolfle, S.M. Qaim, G. Stocklin, Radiochimica Acta 40 (1986) 113.
[20] E. Gidrakos, Chem. Ing. Techn. MS 1301/84 (1984).
[21] C.C. Miles, S. Wexler, E.R. Ebersole, Tritium retention in EBR-II irradiated boron carbide, USAEC Report, Argonne National Laboratory, ANL-8107, 1974.
[22] T. Maruyama, T. Iseki, J. Nucl. Mater. 133&134 (1985) 727.
[23] P. Franzen, B.M.U. Scherzer, W. Moller, Nucl. Instrum. and Meth. B 67 (1992) 536.
[24] Y. Yamauchi, Y. Hirohata, T. Hino et al., J. Nucl. Mater. 220–222 (1995) 851.